Protein Science (1998), 7:185–192. Cambridge University Press. Printed in the USA.

Contaminant inclusion into protein crystals analyzed by electrospray mass spectrometry and X-ray crystallography

JOACHIM HIRSCHLER,[1,2] FRÉDÉRIC HALGAND,[3] ERIC FOREST,[3]
AND JUAN CARLOS FONTECILLA-CAMPS[1]

[1] Laboratoire de Cristallographie et de Cristallogenèse des Protéines, Institut de Biologie Structurale J.-P. Ebel (CEA-CNRS) 41, avenue des Martyrs 38027 Grenoble Cédex 1, France
[2] AEROSPATIALE Espace et Défense 66, route de Verneuil 78133 Les Mureaux Cédex, France
[3] Laboratoire de Spectrométrie de Masse des Protéines, Institut de Biologie Structurale J.-P. Ebel (CEA-CNRS) 41, avenue des Martyrs 38027 Grenoble Cédex 1, France

(RECEIVED June 12, 1997; ACCEPTED October 14, 1997)

Abstract

The inclusion of protein contaminants into crystals of turkey egg white lysozyme (TEWL) was investigated by electrospray mass spectrometry of the dissolved crystals. The results show that significant amounts of the structurally related contaminant hen egg white lysozyme (HEWL) are included in the crystals of TEWL. The structurally unrelated contaminant RNAse A, on the other hand, is not included. The X-ray diffraction data statistics of a hybrid TEWL/HEWL crystal and an uncontaminated TEWL crystal were of similar quality. This indicates that, even though the crystals contain much higher levels of the contaminant than one would have expected after a recrystallization experiment, they are still suitable for X-ray diffraction experiments. However, attempts to detect the presence of the contaminant in the crystal by crystallographic structure refinement did not yield conclusive results.

Keywords: contaminant inclusion; diffraction statistics; mass spectrometry; protein crystal growth; protein crystallography; protein crystal quality; protein impurity; recrystallization

Impurities being an inherent problem to protein crystallization, we have investigated the effects of an added impurity (a contaminant) on protein crystallization and on the quality of the resulting protein crystals. Turkey egg white lysozyme contaminated by hen egg white lysozyme was used (Abergel et al., 1991). This co-crystallization leads to TEWL crystals with a shortened *c*-axis, without changing the original hexagonal symmetry of the crystals (Abergel et al., 1991; Provost & Robert, 1995; Hirschler & Fontecilla-Camps, 1996). This shortening effect is specifically induced by HEWL, a contaminant of closely related structure that only differs from TEWL by 7 of the total 129 residues. Subsequent kinetic measurements have shown that the modified crystal morphology is induced by interactions between HEWL and the crystal surface, reducing the face growth rates of one of the two displayed sets of crystal faces (Hirschler & Fontecilla-Camps, 1997). TEWL solutions were also contaminated by RNAse A (Fontecilla-Camps et al., 1994), a protein similar to TEWL in molecular weight and isoelectric point, but of unrelated three-dimensional structure. These crystals did not show any morphological changes (Hirschler & Fontecilla-Camps, 1996), indicating that the effect of HEWL is specific.

Subsequently, we became interested in the exact composition of the TEWL crystals obtained from HEWL-contaminated solution. Judging from the known procedure of protein recrystallization used to remove protein impurities, we expected a very low degree of HEWL included into the TEWL crystals. Yet chromatographic analysis of TEWL crystals grown from HEWL-contaminated solution had already indicated some contaminant inclusion (Abergel et al., 1991). From final UV-measured protein concentration of equilibrated crystallization droplets, we were able to estimate the extent of this inclusion (Hirschler & Fontecilla-Camps, 1996). According to these preliminary results, the TEWL crystals contain significant amounts of co-crystallized HEWL, which indicates that a recrystallization procedure to separate these two lysozymes would be ineffective. In order to verify these results by a more precise and direct technique, we turned to ESI-MS, a sensitive tool to detect even minor protein inhomogeneities (e.g., Siuzdak, 1994). Preliminary ESI-MS tests to distinguish between the two lysozymes were

Reprint requests to: J.C. Fontecilla-Camps, Laboratoire de Cristallographie et de Cristallogenèse des Protéines, Institut de Biologie Structurale J.-P. Ebel (CEA-CNRS) 41, avenue des Martyrs 38027 Grenoble Cédex 1, France; e-mail: juan@lccp.ibs.fr; or E. Forest, Laboratoire de Spectrométrie de Masses des Protéines, Institut de Biologie Structurale J.-P. Ebel (CEA-CNRS) 41, avenue des Martyrs 38027 Grenoble Cédex 1, France; e-mail: forest@ibs.ibs.fr.

Abbreviations: CSD, charge state distribution; ESI-MS, electrospray ionization mass spectrometry; HEWL, hen egg white lysozyme; RMSD, RMS deviation; RNAse A, ribonuclease A; TEWL, turkey egg white lysozyme.

successful, giving molecular weights of 14,201 ± 1.4 Da for TEWL and 14,305 ± 1.4 Da for HEWL. Subsequently, we started a series of ESI-MS measurements on dissolved HEWL-contaminated TEWL crystals in order to determine directly their HEWL/TEWL ratios. As a control, we also analyzed TEWL crystals from an RNAse A-contaminated solution.

In a next step, we wanted to study the effect of HEWL inclusion on TEWL crystal quality. Previously obtained precession photographs had indicated that HEWL-contaminated TEWL crystals are still capable of diffracting X-rays (Abergel et al., 1991). In a more detailed approach, we have compared the statistics of the X-ray diffraction data from an uncontaminated and a HEWL-contaminated TEWL crystal. Subsequently, we have refined the crystallographic structure against the collected diffraction data from a TEWL/HEWL crystal. Using the obtained electron density maps, we have investigated the contaminant's presence in the crystals.

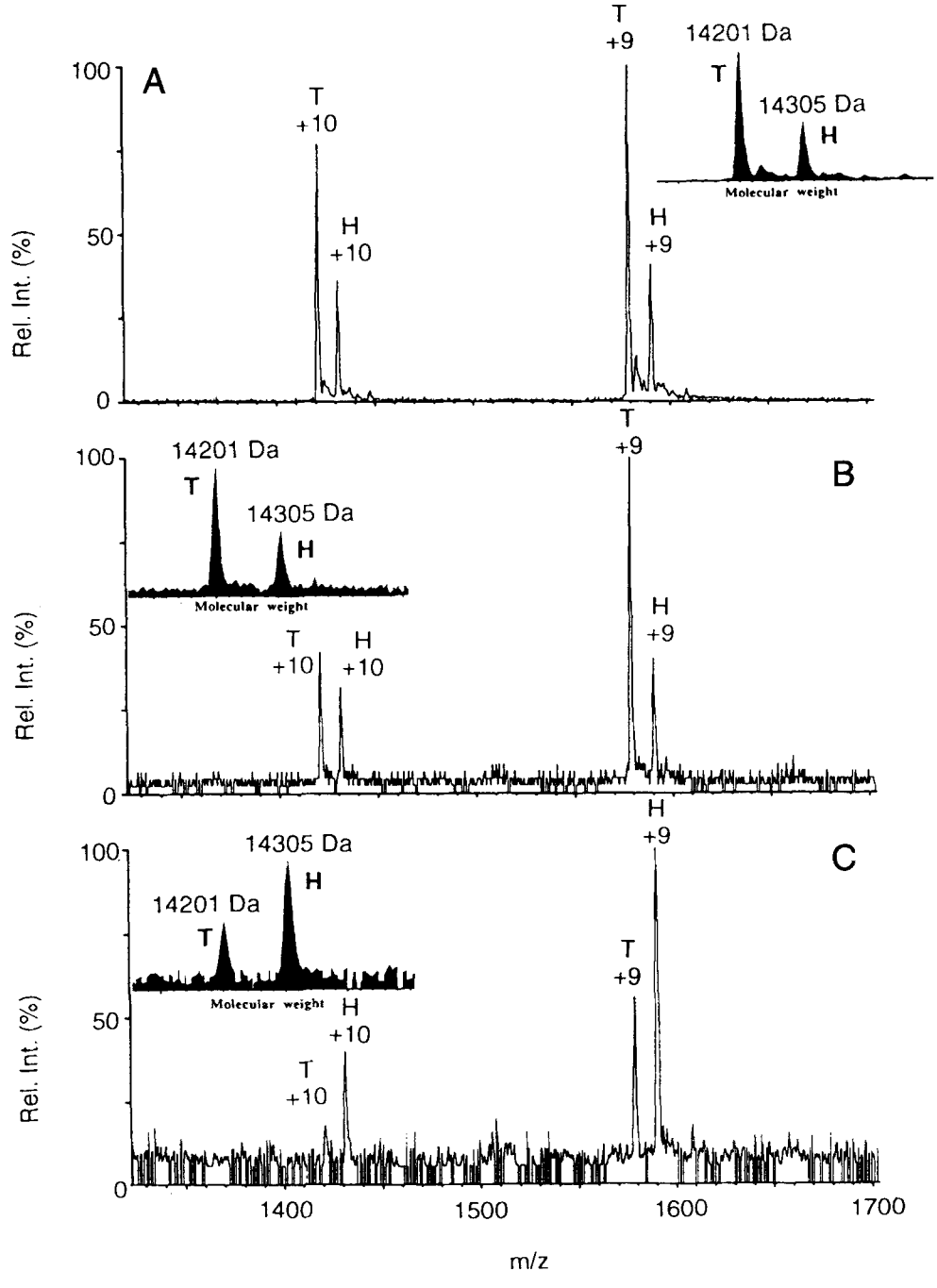

Fig. 1. **A:** ESI mass spectra of the initial TEWL crystallizing solution contaminated by 30% HEWL. **B:** Corresponding spectra of the dissolved crystal shows a HEWL/TEWL ratio almost as high as that in the initial solution. **C:** An even higher supernatant HEWL/TEWL ratio is found in the supernatant (see text). Insets show the reconstructed mass spectra obtained by using a deconvolution algorithm (Perkin-Elmer Sciex).

To our knowledge, this represents the first determination of relative contaminant contents in protein crystals by ESI-MS.

Results

ESI-MS analyses of contaminated crystals

As determined from the reconstructed spectra (Fig. 1), the rinsed and dissolved contaminated crystals analyzed by ESI-MS yielded HEWL/TEWL ratios that were nearly as high as those found in the initial crystallizing solutions, at the four different contamination levels used (Table 1). The subsequent analyses of the supernatants yielded HEWL/TEWL ratios that were significantly higher than those of the initial crystallizing solutions. In the example given in Figure 1, the supernatant solution contained 66% HEWL (Fig. 1C), whereas the initial crystallizing solution had contained 30% HEWL (Fig. 1A). The rinsing solutions, on the other hand, did not contain any HEWL and were therefore not considered in further analyses.

In the case of RNAse A, we recorded the spectra of the protein alone (Fig. 2A) and in the presence of TEWL (Fig. 2B; there are modifications of the RNAse A change state distribution (CSD) due to TEWL). The analysis of a crystal of TEWL contaminated by 30% RNAse A did not reveal any trace of contaminant in the crystals (Fig. 2C). Yet, RNAse A was detected in high concentrations in the corresponding supernatants (Fig. 2D), confirming that the TEWL crystals do not include the RNAse A contaminant.

Using the same ESI-MS protocol, we verified reproducibility and accuracy of the values obtained for the HEWL/TEWL ratios. Taking four TEWL solutions contaminated at different levels from 15% to 37% HEWL (total protein concentration of 30 mg/mL), we repeated each ESI-MS measurement 10 times and calculated for each of the four solutions the corresponding RMSD. As can be seen from Table 2, the RMSDs are small compared to the experimental results and do not vary systematically with the HEWL/TEWL ratio.

X-ray diffraction results and model refinement

The TEWL crystal obtained in the presence of 32% HEWL diffracted to 2.1 Å resolution with $\langle I \rangle / \sigma(I) = 9.7$ (Table 3). The diffraction statistics compare well to those of an uncontaminated TEWL crystal; only its R_{sym} being somewhat higher. Also, its cell parameters ($a = b = 71.9$ Å, $c = 85.5$ Å, $\alpha = \beta = 90°$, $\gamma = 120°$) agree closely with those of the uncontaminated TEWL crystals ($a = b = 73.2$ Å, $c = 86.8$ Å). Both crystals belong to the hexagonal space group $P6_122$ (see also Hirschler & Fontecilla-Camps, 1996). The final refined model contains 129 residues and 51 water molecules and has good stereochemistry. Four Arg side chains situated on the molecular surface are ill-defined. The free *R*-factor of the model is 0.26%.

Examination of the electron density map at the seven positions where the two lysozymes differ did not give conclusive results for the contaminant's presence. For example, there is no electron density around Gly 101, which is replaced by Asp 101 in HEWL. However, some indications suggest the contaminant's presence. An example is the $2F_o - F_c$ omit map around residue Tyr 3. Using a 1.0σ cut-off, the phenyl ring as well as the hydroxyl oxygen atom are well accounted for by the experimental electron density. When the cut-off is increased to 1.2σ, the hydroxyl oxygen lays outside the electron density (Fig. 5A). This is compatible with the contaminant's inclusion having partially replaced TEWL Tyr 3 → HEWL Phe 3. As a control, we examined Tyr 23, which is conserved in HEWL. When the σ cut-off of the $2F_o - F_c$ omit map is increased in the same manner, the electron density still accounts for the hydroxyl oxygen of Tyr 23. These observations hint at the HEWL presence in the crystals (Fig. 5B).

Discussion

ESI-MS experiments

The ESI-MS experiments are reproducible and well adapted to determine the relative HEWL content of the crystals and the supernatants. This can be seen from the low RMSDs of the 10-fold repeated measurements of TEWL solutions contaminated at different levels with HEWL (Table 2). Although the ionization–desorption process of proteins in aqueous solution in the electrospray source is still a subject of debate (e.g., Kebarle & Tang, 1993), it is clear that the relative intensities of the respective charge states of two very similar proteins (similar structures and CSDs) acquired on the same spectra are representative of the proteins' relative concentrations. This is illustrated by the TEWL/HEWL spectra compared to the TEWL/RNAse A spectra (Figs. 1, 2). In the first case, no modification of the CSD was observed when compared to

Table 1. *Relative percentages of HEWL and of RNAse A in TEWL crystals (w/w total protein) and in supernatants at different contamination levels in the initial crystallizing solution (respective SD for averaged values in parentheses) determined by ESI-MS*

	Contaminant content in		
	Initial solution (%)	Crystals (%)	Supernatants (%)
HEWL	16	13.5 (2.1)	46 (1.7)
HEWL	22.5	18 (0)	55 (0)
HEWL	32	24 (6.2)	66 (2.6)
HEWL	37.5	31.5 (5.8)	68 (2.9)
RNAse A	30	No trace	—

Table 2. *Verification of reproducibility of ESI-MS measurements on TEWL solutions contaminated by HEWL*[a]

Series	Average HEWL content (%)	RMSD
1	14.8	1.40
2	21.0	1.00
3	30.0	1.33
4	37.0	1.49

[a]RMSDs of HEWL/TEWL ratios determined by ESI-MS for four different HEWL/TEWL solutions (ranging from 15% to 37% HEWL, 10 consecutive ESI-MS measurements for each of the four series).

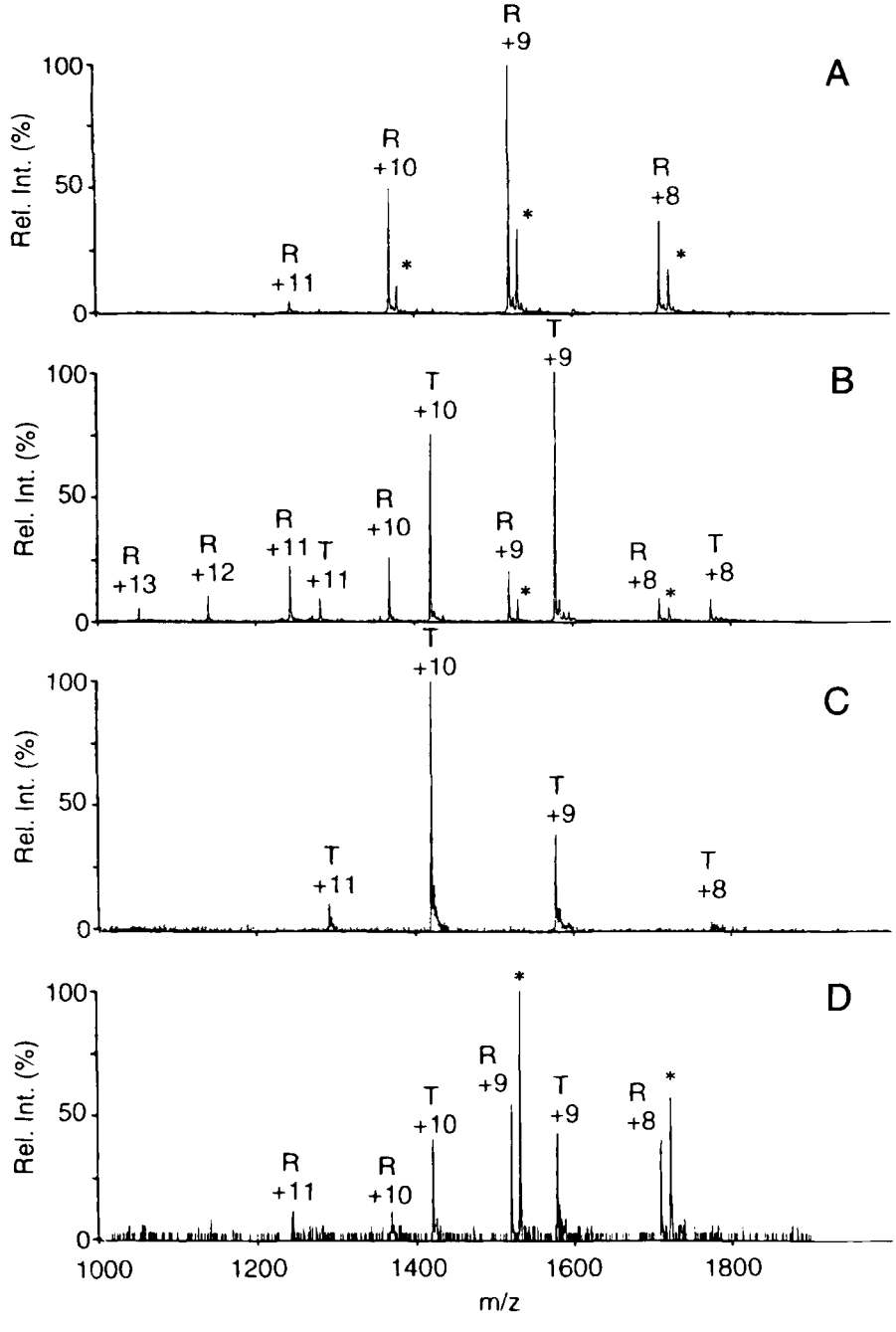

Fig. 2. ESI mass spectra of RNAse A alone (**A**) and of the TEWL crystallizing solution contaminated with 30% RNAse A (**B**). RNAse A is not found in the crystal samples (**C**), whereas it is observed in the supernatants (**D**). The phosphate-bound form of RNAse A is marked by * in the spectra.

the CSD of the spectra of TEWL and of HEWL alone. The CSD of RNAse A, on the other hand, undergoes a change when acquired in the presence of TEWL (whereas the CSD of TEWL is not affected). This result can be explained by a modified ionization–desorption process in the mixed solution due to the different properties of the two proteins. The experimental RMSDs observed for the HEWL/TEWL ratios (up to 6.2 for 24% HEWL in the crystals, Table 1) may be explained by the experimental conditions of crystal growth and sample preparation. These deviations are not due to the methodology itself, as shown by the RMSDs reported in Table 2.

Using calibration curves derived from internal protein standards (e.g., methylated lysozymes) may allow not only determination of the relative amount of HEWL (the HEWL/TEWL ratio) in the crystals, but also quantification of the amount in absolute terms. This, however, was not the aim of our study.

Crystal contaminant inclusion

The HEWL/TEWL ratio of the crystals is very high and it comes close to the one in the initial crystallizing solution (Table 1). This

is shown by ESI-MS analyses of crystals grown from solutions contaminated from 16% to 37.5% HEWL. The averaged HEWL/TEWL ratio in the crystals is always slightly lower than that in the corresponding initial solution. This also confirms our previously obtained preliminary data on HEWL inclusion into TEWL crystals from UV measurements (Hirschler & Fontecilla-Camps, 1996). Using a linear approximation for the HEWL inclusion determined by ESI-MS as a function of initial HEWL percentage in solution, we obtain a slope of 0.80 (Fig. 3). This tells us that the HEWL/TEWL ratio in the crystals corresponds to approximately 80% of that present in the initial solutions. The crystals include the principal component TEWL and the contaminant HEWL, with very little segregation during their growth. As a first approximation, the HEWL/TEWL ratio in the crystals therefore simply corresponds to the HEWL/TEWL ratio in the crystallizing solution. The contaminant inclusion is much higher than what could be expected after a recrystallization procedure (e.g., McPherson, 1989; McRee, 1993). Such a procedure to separate the two lysozymes therefore would have been ineffective. Yet, because we found no signs of RNAse A included in the TEWL crystals, a recrystallization would have successfully separated TEWL from this contaminant, which is structurally unrelated. These results also confirm our hypothesis that only the structurally related contaminant HEWL can be included in the crystal lattice of TEWL. Despite their high degree of inclusion, the TEWL/HEWL crystals are as well-developed as the TEWL crystals obtained from RNAse A-contaminated solutions (Fig. 4). We have correlated the similarity of the contaminant's structure first to its influence on the crystal habit (Abergel et al., 1991; Hirschler & Fontecilla-Camps, 1996) and then to its inclusion in the crystals. The coexistence of the two aspects in our case, however, is not a general phenomenon, and they are not at all necessarily linked.

As mentioned above, the HEWL concentration in the final supernatant exceeds that of the initial solution. This is explained by the fact that the HEWL inclusion in the crystals does not correspond exactly to the HEWL/TEWL ratio in solution, but that it is slightly lower. During crystal growth, the concentration of HEWL relative to TEWL is thus continuously increasing in the supernatant. The lower the TEWL concentration is in solution, the higher this enrichment is in relative terms. This continues until the equilibrium TEWL concentration is reached. We have modeled this behavior by a series of simple calculations. From known crystallization droplet parameters and TEWL solubility (1.6 mg/mL, Hirschler & Fontecilla-Camps, 1996), we can calculate the final HEWL supernatant concentration. For a TEWL solution with 16% initial HEWL, for example, we come up with a final HEWL percentage of 41% (see Materials and methods). The corresponding experimental value is 45.5%. The high supernatant HEWL/TEWL ratios (Fig. 3) are thus fully explained by these calculations.

X-ray data collection and structure refinement of HEWL-contaminated TEWL crystal

In spite of the high degree of HEWL inclusion into the TEWL crystals, the hybrid crystals gave X-ray diffraction statistics comparable to those of uncontaminated ones. This suggests that HEWL packs well into the TEWL crystal lattice, a result that may be explained by the similar three-dimensional structure of the contaminant. Examination of the usual difference electron density maps calculated with the final model phases did not furnish clear-cut evidence for the contaminant's presence. Reducing the model bias by calculating omit maps for the mutated residue positions gave some indications for this (see Fig. 5A,B), but did not yield conclusive results either. It is possible that the lack of electron density for several of the HEWL-specific residues results from the relatively low concentration of contaminant in the crystal, which, according to our ESI-MS experiments, was approximately 27%. Higher-resolution data may also be instrumental in getting a better representation of the hybrid electron density at the HEWL-specific residues. Experiments at a synchrotron radiation source are in progress.

Conclusion

Using ESI-MS, the degree of contaminant inclusion into TEWL crystals upon co-crystallization has been shown to be very significant for the HEWL contaminant, and negligible for the RNAse A contaminant. The crystallization of TEWL in the presence of HEWL results in HEWL/TEWL hybrid crystals. The HEWL/TEWL ratio observed in the crystals is approximately 80% of the one in the initial crystallizing solution, indicating that the inclusion of HEWL into TEWL crystals is mainly a function of the composition of the crystallizing solution. Trying to recrystallize the two lysozymes to

Table 3. *Data collection statistics and crystal parameters of a crystal obtained from TEWL solution contaminated by 32% HEWL (w/w of total protein) compared to the data of a TEWL crystal from uncontaminated solution*

	TEWL contaminated by HEWL	TEWL uncontaminated
Resolution (Å)	2.1	2.3
Number of observations	73,102	31,795
Number of reflections	7,442	5,872
R_{sym} (%)	9.8	7.2
Completeness (%)	92.7	99.8
For last shell (%)	2.24–2.11 Å: 60.9	2.44–2.34 Å: 41.2
Redundancy	9.8	5.41
$I/\Sigma(I)$	9.7	15.9
Cell dimension (Å)	$a = b = 71.9$, $c = 85.5$	$a = b = 73.2$, $c = 86.8$
Space group	$P6_122$	$P6_122$

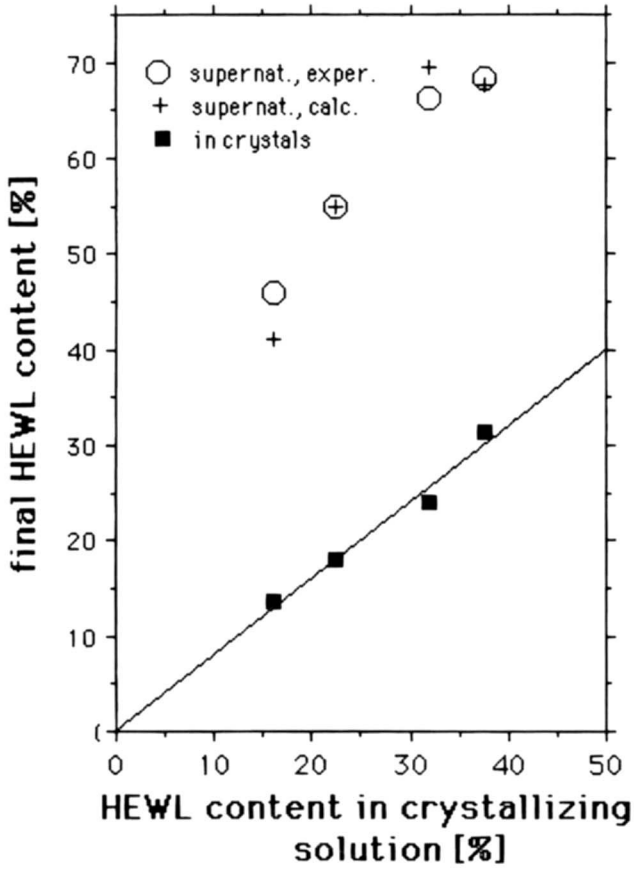

Fig. 3. HEWL percentages detected in TEWL crystals by ESI-MS as a function of HEWL contamination in the initial crystallizing solution (squares: HEWL in crystals). Crystals contain almost as much HEWL as the initial crystallizing solution (the slope of the linear least-squares approximation is 0.80). The high final HEWL percentages in the supernatants (circles) are due to enrichment during growth, which can be correctly modeled by calculations (crosses).

separate them from each other therefore would have been inefficient. Despite their high level of HEWL inclusion, the hybrid TEWL/HEWL crystals are well-developed and one of them produced good X-ray diffraction data. Obviously, the high contaminant concentration in the crystals does not affect the X-ray diffracting power. In our study, we have not been able to show clear-cut hybrid electron density at the HEWL-specific residues. We believe this is due to the combined effect of relatively low contaminant concentration in the crystals and not high enough resolution of the data. These problems may be overcome by using higher levels of contamination and a synchrotron radiation source (work in progress).

Materials and methods

Crystals with different contaminant levels

TEWL was used as purchased (Sigma, crystallized, dialyzed, and lyophilized), and HEWL was filtered three times over 3-kDa filter membranes (Microsep 3K for 8 h at 6,000$*g$) prior to use to remove low-molecular weight impurities. Weighed TEWL samples were dissolved in water to a concentration of 30 mg/mL. HEWL

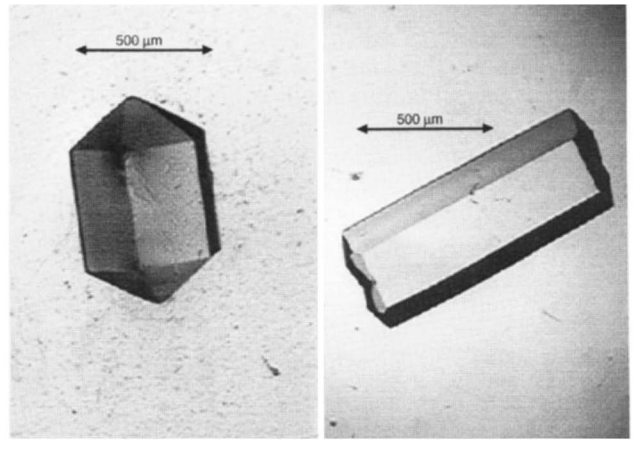

Fig. 4. TEWL crystals grown from solution contaminated by 32% HEWL (left) and from RNAse A-contaminated solution (30%, right). Despite its high HEWL inclusion, the TEWL/HEWL crystal is as well developed as the TEWL crystal, which did not include RNAse A.

concentrations were determined by UV absorbance measurements using a previously established calibration curve. The TEWL solutions were then contaminated by HEWL (total TEWL + HEWL concentration of 30 mg/mL). The exact HEWL/TEWL ratios were determined by ESI-MS (see below). TEWL crystals were grown in the presence of 16, 22.5, 32, and 37.5% (w/w of total protein) HEWL by the vapor-diffusion method at 20 °C in sitting drops of 2 μL of 30 mg/mL total protein and of 2 μL precipitant solution in Linbro plates as published previously (Hirschler & Fontecilla-Camps, 1996). The precipitant solution consisted of 2.40 M NaCl, 0.1 M HEPES buffer (*N*-[2-hydroxyethyl]piperazine-*N'*-[2-ethanesulfonic acid], Fluka BioChimica), pH 5.8, and 15 mM NaN_3 added as an antibacterial agent. A reservoir volume of 1 mL of the precipitant solution was used. Several drops for each crystallization condition were set up. After one week, the supernatants of the crystallization droplets were carefully removed for ESI-MS measurements without touching the crystals (Table 1, "Supernatants"). The crystals remaining on their sitting-drop supports were rinsed five times with 5 μL of the precipitant solution to avoid cracking of the crystals and transferred to Eppendorf tubes ("Initial solution"). The crystals were then transferred, along with a small aliquot of the precipitant solution, into Eppendorf tubes and dissolved by strong agitation ("Crystals"). The same protocols were applied to crystals obtained from TEWL solutions contaminated by 30% (w/w total protein) RNAse A [at 30 mg/mL total protein concentration; RNAse A purified as described in Fontecilla-Camps et al. (1994)].

ESI-MS experiments

Mass spectrometry measurements were performed using a Sciex API III + triple quadrupole mass spectrometer (Perkin-Elmer Sciex, Canada) equipped with a nebulizer-assisted electrospray source. The instrument was calibrated using polypropylene glycol. Mass spectra were acquired by flow injection analysis using a solution of 25% (v/v) methanol and 1% (v/v) acetic acid in water as the infusing solvent. A 1,200–1,900 mass-to-charge (m/z) ratio was used, with steps of 0.5 (m/z) for a dwell time of 3 ms. When

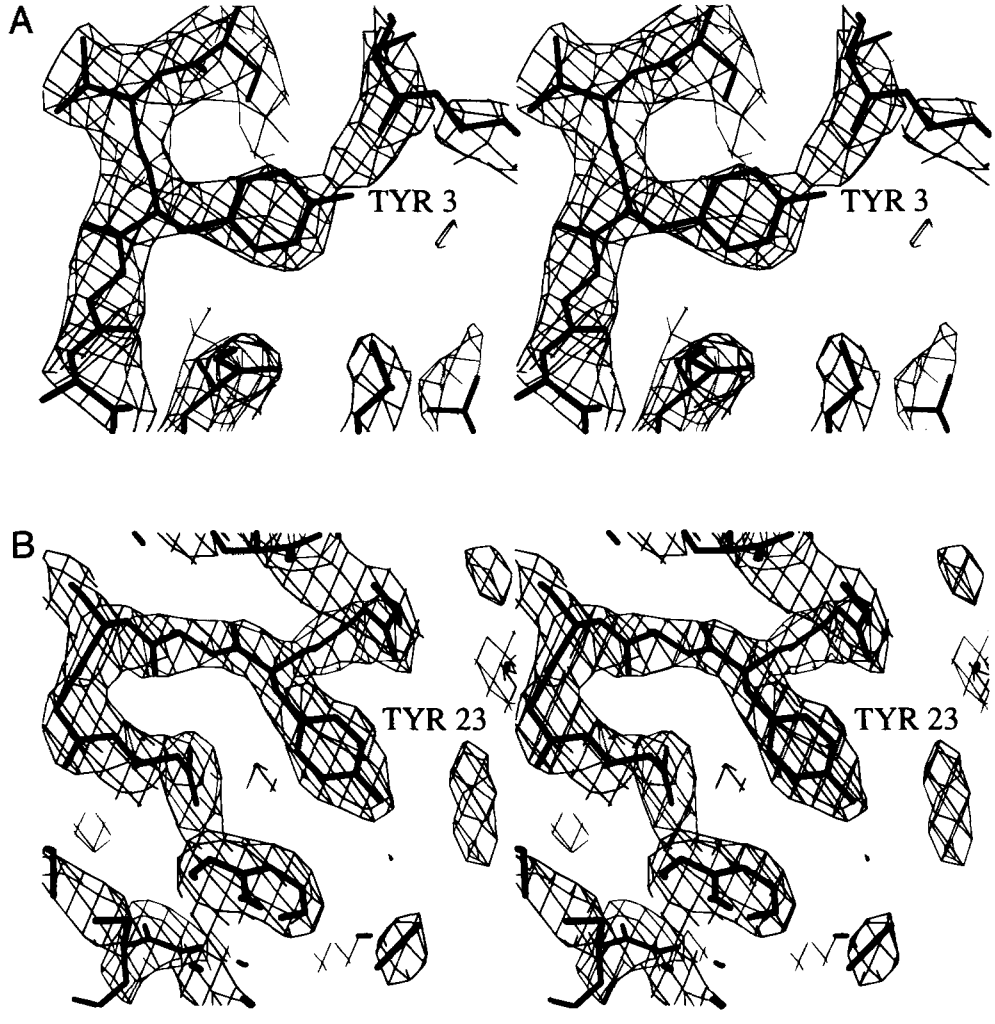

Fig. 5. Superposition of the final TEWL model on the $2F_o - F_c$ omit electron density maps contoured at 1.2σ around Tyr 3 (**A**) and Tyr 23 (**B**). Increasing the cut-off from 1.0 to 1.2σ, the hydroxyl-O of Tyr 3 lays outside the electron density. This is compatible with the TEWL Tyr 3 → HEWL Phe 3 replacement lowering the electron density around hydroxyl-O. In the case of Tyr 23 (conserved in HEWL), the electron density still accounts for the hydroxyl-O after increasing the σ cut-off to 1.2. These observations hint at the contaminant's presence in the crystal.

necessary, samples were diluted to 20 pmol/μL before injection. The problem of high salt concentration in the samples was solved by acquiring the spectra using a collision-activated dissociation at the interface of the electrospray. The removal of part of the ions was thus achieved by varying the orifice voltage from 80 V to 110 V.

Diffraction data collection

Both hybrid TEWL/HEWL and the uncontaminated TEWL crystals were mounted in 0.7-mm diameter glass capillaries. X-ray diffraction data were collected on a Xentronics/Siemens area detector coupled to a Rigaku RU 200 generator, running at 50 kV and 100 mA, with a graphite monochromator at 25 °C. The reflections were processed, scaled, and reduced with the program package XENGEN (Howard et al., 1987). For the structure refinement of the hybrid crystal, a previously published TEWL crystal structure (PDB code 2lz2, Bott & Sarma, 1976) was taken as the initial model. This model was refined against the diffraction data initially using the standard simulated-annealing procedure of the program X-PLOR (Brünger, 1992). This was followed by several cycles of energy minimization and of individual *B*-factor refinement. The model was graphically modified using the program O (Jones et al., 1991) according to electron density maps calculated with $2F_o - F_c$ and $F_o - F_c$ coefficients. Water molecules were built only in plausible hydrogen bonding positions. Omit maps were calculated for each of the seven HEWL-specific residues in order to remove bias from the electron density calculated with model phases.

Calculating HEWL supernatant concentration

For example, in the case of a 2-μL drop of 30 mg/mL protein solution at 16% HEWL, we can estimate the initial TEWL and HEWL amounts to be 0.0504 mg and 0.0096 mg, respectively. Based on the reported TEWL solubility (Hirschler & Fontecilla-Camps, 1996), we know that 0.0032 mg of TEWL will stay in

solution, whereas 0.0472 mg will crystallize. From the ESI-MS analysis, we have determined that the crystal contains 13.5% HEWL, corresponding to 0.0074 mg. Thus, 0.0022 mg of the protein remain in solution. Because the soluble TEWL contribution is equal to 0.0032 mg, the relative HEWL content is 41% (neglecting the contribution of the HEWL solubility). The corresponding experimental value is 45.5%.

Acknowledgments

We thank Dr. Mitsuo Ataka of the National Institute of Bioscience and Human Technology in Tsukuba, Japan, for stimulating comments on the inclusion of contaminants, especially with respect to the RNAse A contaminant.

References

Abergel C, Nesa MP, Fontecilla-Camps JC. 1991. The effect of protein contaminants on the crystallization of turkey white lysozyme. *J Crystal Growth 110*:11–19.

Bott R, Sarma R. 1976. Crystal structure of turkey egg-white lysozyme—Results of the molecular replacement method at 5 Å resolution. *J Mol Biol 106*:1037–1046.

Brünger AT. 1992. *X-PLOR version 3.1, a system for X-ray crystallography and NMR*. New Haven, Connecticut/London: Yale University Press.

Fontecilla-Camps JC, de Llorens R, le Du MH, Cuchillo CM. 1994. Crystal structure of ribonuclease A*d(ApTpApApG) complex. *J Biol Chem 269*: 21526–21531.

Hirschler J, Fontecilla-Camps JC. 1996. Contaminant effects on protein crystal morphology in different growth environments. *Acta Crystallogr D 52*:806–812.

Hirschler J, Fontecilla-Camps JC. 1997. Protein crystal growth rates are face-specifically modified by structurally related contaminants. *J Crystal Growth 171*:559–565.

Howard AJ, Gilliland GL, Finzel BC, Poulos TL, Ohlendorf DH, Salemme FR. 1987. The use of an imaging proportional counter in macromolecular crystallography. *J Appl Crystallogr 20*:383–387.

Jones TA, Zou JY, Cowan SW, Kjeldgaard M. 1991. Improved methods for building protein models in electron density maps and the location of errors in these models. *Acta Crystallogr A 47*:110–119.

Kebarle P, Tang L. 1993. From ions in solution to ions in the gas phase—The mechanism of electrospray mass spectrometry. *Anal Chem 65*:972–986.

McPherson A. 1989. *Preparation and analysis of protein crystals*. Malabar, Florida, USA: Krieger Publishing Company.

McRee DE. 1993. *Practical protein crystallography*. San Diego, California: Academic Press.

Provost K, Robert MC. 1995. Crystal growth of lysozymes in media contaminated by parent molecules: Influence of gelled media. *J Crystal Growth 156*:112–120.

Siuzdak G. 1994. The emergence of mass spectrometry in biochemical research. *Proc Natl Acad Sci USA 91*:11290–11297.